Gas phase detection and rotational spectroscopy of ethynethiol, HCCSH

Kin Long Kelvin Lee,[*,†] Marie-Aline Martin Drumel,[‡] Valerio Lattanzi,[¶] Brett A. McGuire,[§,†] Paola Caselli,[¶] and Michael C. McCarthy[†]

†*Harvard-Smithsonian Center for Astrophysics, 60 Garden Street, Cambridge MA 02138, USA*

‡*Institut des Sciences Moléculaires d'Orsay, CNRS, Univ Paris Sud, Université Paris-Saclay, Orsay, France*

¶*The Center for Astrochemical Studies, Max-Planck-Institut für extraterrestrische Physik, Garching, Germany*

§*NAASC, National Radio Astronomy Observatory, Charlottesville VA 22903, USA*

E-mail: kinlee@cfa.harvard.edu

Abstract

We report the gas-phase detection and spectroscopic characterization of ethynethiol (HCCSH), a metastable isomer of thioketene (H_2C_2S) using a combination of Fourier-transform microwave and submillimeter-wave spectroscopies. Several *a*-type transitions of the normal species were initially detected below 40 GHz using a supersonic expansion-electrical discharge source, and subsequent measurement of higher-frequency, *b*-type lines using double resonance provided accurate predictions in the submillimeter region. With these, searches using a millimeter-wave absorption spectrometer equipped with a radio frequency discharge source were conducted in the range 280 – 660 GHz, ultimately yielding nearly 100 transitions up to ${}^rR_0(36)$ and ${}^rQ_0(68)$. From the combined data set, all three rotational constants and centrifugal distortion terms up to the sextic order were determined to high accuracy, providing a reliable set of frequency predictions to the lower end of the THz band. Isotopic substitution has enabled both a determination of the molecular structure of HCCSH and, by inference, its formation pathway in our nozzle discharge source via the bimolecular radical-radical recombination reaction SH+ C_2H, which is calculated to be highly exothermic (-477 kJ/mol) using the HEAT345(Q) thermochemical scheme.

Introduction

From a fundamental perspective, the structure and properties of small organosulfur molecules have long fascinated theorists[1–4] and experimentalists alike.[5,6] Much of this interest stems both from the large number of minima on the potential energy surface that are predicted to exist even when the molecule consists of a relatively small number of atoms, and from the multitude of distinct reaction pathways that might preferentially produce these isomers. Interest in small organosulfur molecules has only intensified in recent years, driven by the discovery that small, hydrogen-deficient sulfur bearing molecules such C_2S and C_3S are ubiquitous in cold molecular clouds and other astronomical sources. In contrast, their

hydrogen-terminated counterparts appear conspicuously absent.

Organosulfur molecules with the [H_2, C_2, S] formula are one such example. As many as six different stable, singlet isomers have been predicted, with roughly twice that number of triplet variations.[7] Although the stability and relative ordering of the highest energy isomeric arrangements is not fully resolved, there is a general consensus from the electronic structure calculations as to the ordering of the three lowest-energy isomers (Fig. 1): thioketene (H_2CCS), the most stable and the most extensively studied isomer;[8–10] ethynethiol (HCCSH), the thioenol form predicted here to lie roughly 60 kJ/mol higher in energy; and thiirene (c-H_2C_2S), the three-membered heterocycle lying ∼135 kJ/mol above the ground state.[7] Due to their high reactivity, the latter two species have remained somewhat enigmatic in the laboratory. While both are known to form from the decomposition of thiadazoles under ultraviolet irradiation in an argon matrix,[5,6,8,11] the intermediate steps that allow isomerization between the three species remain unclear, despite their importance as potential intermediates in chemical synthesis[12] and photochemistry.[13,14] These metastable isomers may also be of astronomical interest because formation pathways in the interstellar medium are kinetically, not thermodynamically-controlled, and, as a result, dramatic departures from equilibrium often occur, as evidenced from the presence of high-energy isomers in a wide range of astronomical objects.[15]

Other organosulfur species, specifically the cumulenic C_nS[16–18] and H_2C_nS chains,[19] and the HC_nS free radicals,[20] have been extensively studied by rotational spectroscopy, largely motivated by their possible astronomical interest. A by-product of these studies has been precise molecular structures and in some cases detailed information on the electronic distribution. Because small sulfur species, such as H_2S, only account for a small fraction of the available sulfur in these molecular clouds, it has been widely theorized that the 'missing' sulfur is sequestered in either the condensed phase or in yet undetected sulfur-bearing molecules. For this reason, astronomical searches for new organosulfur species are often undertaken once accurate rotational line frequencies become available.

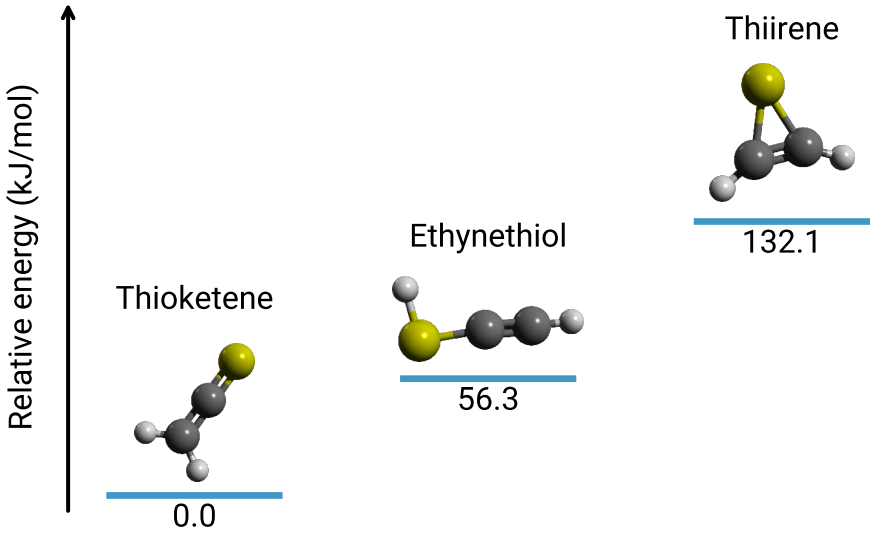

Figure 1: Relative energies of the [H_2,C_2,S] isomers determined with the composite thermochemistry method outlined in the text. Energies are computed at 0 K, given in kJ/mol, and are relative to the lowest energy form, H_2CCS.

Driven by a desire to better understand the low-lying isomers of small organosulfur species, and to identify possible new transient species that might serve as attractive 'sinks' for sulfur in molecular clouds, rotational spectroscopy and high-level theoretical calculations have been undertaken on the [H_2,C_2,S] isomeric system. Particular emphasis is placed on the second most stable isomer HCCSH, because it plausibly might form directly and efficiently via a recombination reaction[7] involving two well-known astronomical radicals, SH and CCH. To fully characterize its rotational spectrum, measurements have been made both at centimeter wavelengths using Fourier transform (FT) microwave spectroscopy and at submillimeter wavelengths using a frequency multiplication spectrometer. To gain insight into the formation pathway of HCCSH in our discharge nozzle source, isotopic investigations have been performed using isotopically-enriched precursors. To compliment this study, thermochemical calculations using the HEAT protocol have been made to establish the exothermicity of the SH + CCH reaction, and more accurately determine the relative stability of the lower-lying [H_2,C_2,S] isomers. A by-product of the isotopic measurements is a determination of a semi-experimental (r_e^{se}) structure for HCCSH. This structure is discussed in comparison to purely

equilibrium ones predicted from coupled cluster calculations.

Experimental and computational methods

Quantum-Chemical Calculations

Calculations were performed using the CFOUR suite of electronic structure programs.[21] Unless otherwise specified, all-electrons (ae) are correlated in the post-Hartree-Fock (HF) calculations, using coupled cluster methods with single, double, and perturbative triple [CCSD(T)][22–24] excitations and correlation consistent basis sets with core-valence basis functions (cc-pCVXZ)[25,26] and without (cc-pVXZ)[27] of double (X = D), triple (X = T), and quadruple (X = Q) zeta quality. Accurate predictions of the equilibrium structure of HCCSH were obtained by performing geometry optimizations using CCSD(T)/cc-pCVXZ (X = D, T, Q), and the various spectroscopic parameters (e.g. equilibrium rotational constants, quartic centrfigual distortion constants) calculated with the cc-pCVQZ geometry. First order vibration-rotation interaction constants required for a semi-experimental molecular structure were calculated under the frozen-core approximation with fc-CCSD(T)/ANO0.

To estimate the reaction thermochemistry, we performed HEAT345(Q) calculations which routinely yield chemical accuracy ($\sim$1 kJ/mol).[28,29] Since the scheme has been described in previous publications, we only briefly outline it here. Using the CCSD(T)/cc-pVQZ geometry, a series of additive contributions are calculated, including: complete-basis set (CBS) extrapolations of correlation energy using CCSD(T)/aug-cc-pCVXZ (X = T, Q, 5); the harmonic zero-point energy (CCSD(T)/cc-pVQZ); extrapolated corrections to the perturbative triple excitations [T - (T)];[30] the diagonal Born-Oppenheimer correction (DBOC) with HF/aug-cc-pVTZ;[31] scalar relativistic corrections [CCSD(T)/aug-cc-pCVTZ];[32,33] and quadruple excitations [fc-CCSDT(Q)/cc-pVDZ].[34] The contributions to the total composite energy used to calculate the total HEAT345(Q) energy are given in Table 3

For completeness, the relative energetics of the lower-lying [H_2,C_2,S] isomers, have also

been re-calculated with a lower level of computation sophistication. For these calculations, the [T - (T)] term has been omitted, and due to linear dependence in the largest basis used for the correlation calculations on c-H_2C_2S, the extrapolated CCSD(T)/CBS calculations utilized the cc-pCVXZ (X = T, Q, 5) basis sets instead of their augmented variants are used in the HEAT345(Q) treatment.

Fourier-transform microwave spectroscopy

Experiments at centimeter-wavelengths were conducted first in Cambridge using a FT microwave spectrometer that has been extensively described in previous publications.[35] To produce HCCSH, acetylene (HCCH; 5% in Ne) and hydrogen sulfide (H_2S; 2% in Ne) were mixed in-line and further diluted by tenfold with Ne at a backing pressure of 2.5 kTorr. The mixture was introduced along the axis of a microwave cavity via a discharge nozzle operating at 5 Hz. This nozzle source is electrically isolated from the large aluminum cavity mirror on which it is mounted, and, by means of a small hole near the center of the mirror, the gas mixture adiabatically expands into the large vacuum chamber. By applying a voltage potential between the two cylindrical copper electrodes (1.2 kV) in the discharge stack, many collisions with electrons, atoms, and precursor molecules and its fragments occur prior to adiabatic expansion, yielding a rich broth of familiar and exotic molecules. As the gas reaches the beam waist of the cavity, a pulse of resonant microwave radiation polarizes the plasma. The resulting free-induction decay is detected with a sensitive microwave receiver, the Fourier-transform of which yields the frequency spectrum. Powerful and flexible in-house software is used to control, optimize, and acquire data in the 5 – 40 GHz frequency range of this spectrometer. For isotopic measurements, isotopically-enriched precursors gases such as D_2S, DCCD, $H^{13}C^{13}CH$, etc., were used instead of the normal sample at the same level of dilution.

Once candidate a-type lines of HCCSH were identified, subsequent high-frequency, b-type transitions were sought using double resonance, since these lines are predicted to lie well

above the frequency ceiling of the microwave cavity. In this type of experiment, the cavity spectrometer is tuned to the frequency of a low-J, a-type line, and radiation generated from an active multiplier chain in combination with a second synthesizer is aligned to intersect the beam waste of the cavity. The frequency of this second radiation source is sequentially stepped in small intervals (typically 0.1 MHz) so as to cover the frequency range predicted for the transition. A significant decrease in line intensity is normally observed when the two rotational transitions share a common upper or lower rotational level owing to loss of coherence. Although many hundreds or even thousands of steps may be required to detect these lines, wide frequency sweeps – covering a GHz or more – are readily performed under computer control.

Millimeter-wave spectroscopy using frequency multiplication chains

The submillimeter experiments were performed in Orsay in the 280 – 660 GHz region using a frequency multiplication absorption spectrometer.[36] Briefly, the radiation from a post-amplified synthesizer (7.8 – 12.2 GHz) drives a commercial frequency multiplier source (Virginia Diodes, Inc.). An off-axis parabolic mirror collimates the radiation from the multiplication chain into a 1.2 m long single path Pyrex absorption flow cell equipped with teflon windows, and the output radiation is focused onto a liquid-helium cooled Si-bolometer detector. The flow cell is equipped with a radio frequency resonator driven by a generator that can provide as much as 100 W.[37] In the present experiment, the gas flow was maintained by a mechanical pump. Typical experimental conditions consisted of a 10 W radio frequency discharge; a flowing mixture of HCCH and H_2S in a 1:1 pressure ratio at a total pressure of 50 µbar; a 30–50 kHz frequency step size; a 49 kHz frequency modulation (resulting in a second derivative line shape of the recorded transitions) with a modulation depth of 450 kHz; and a 200 ms time constant. Under these conditions, strong transitions —mainly $K_a'' = 0$ b-type lines— of HCCSH at 300 K fall within the range of the spectrometer. In total, lines were recorded with J'' values ranging from 1 to 68, all with a SNR ratio that was sufficiently

high to determine line centers to 50 kHz accuracy. We note that frequency coverage was limited by the output of the active multiplier chain units, rather than the temperature of our sample.

Results and discussion

On the reliability of the *ab initio* structure determination and dipole moment

The rotational constants and projections of the dipole moment derived with each basis set are reported in Table 1, while the structural parameters obtained at the largest basis (cc-pCVQZ) is shown in Figure 2. Regardless of the basis set, the calculations consistently predict that HCCSH is a near-prolate asymmetric top (asymmetry parameter, $\kappa = -0.999$), with a heavy atom linear backbone nearly coincident with the a inertial axis. Since the S–H bond is close to perpendicular with respect to the heavy backbone, the a and b components of the electric dipole moment are both non-zero, and the A rotational constant is significantly larger than B and C ($\sim$290 GHz compared to roughly 5 GHz).

By performing systematic geometry optimizations, it is possible to assess the convergence of the rotational constants and dipole moments with increasing size of correlation consistent basis sets. As summarized in Table 1, the dipole moments converge quickly with the size of the basis set although the relative change is different for μ_a and μ_b: the former increases with increasing basis, while the latter decreases. The magnitudes of the two moments can be rationalized in the following way: μ_b is dominated simply by the polarity of the S–H bond since all the other atoms in HCCSH lie very close to the a inertial axis. For this reason it is perhaps not surprisingly that the value of μ_b calculated here (μ_a=0.80 D) is very similar to that measured for free SH (μ=0.758 D; Ref. 38). The magnitude of μ_a is more subtle. The CCS radical is calculated to be highly polar (2.8 D; Ref. 39) but, in contrast to HCCSH, possesses a cumulenic :C=C=S: like-structure with formally a lone pair on both the terminal

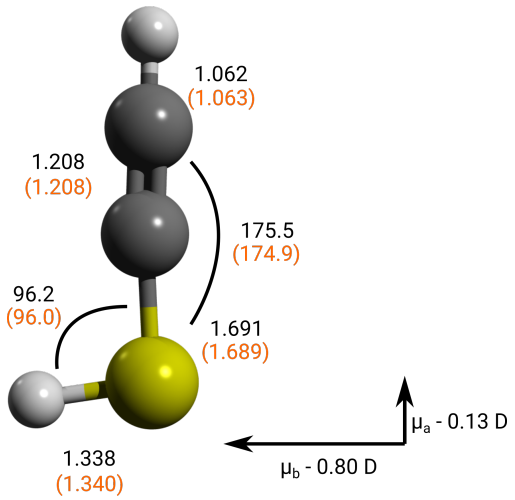

Figure 2: Equilibrium structure of HCCSH computed at the ae-CCSD(T) level of theory. Bond lengths are given in Å, angles in degrees. Values in black (without the parentheses) are obtained with core-valence basis functions (cc-pCVQZ), while the orange parameters correspond to the best-fit semi-experimental parameters (Table 4). Dipole moments (in Debye) are calculated using the CCSD(T)/cc-pCVQZ structure at the same level of theory.

carbon and sulfur atoms. Addition of an H atom to the terminal C fundamentally alters this bonding, imparting an acetylenic-like conjugation to the heavy atom backbone. The absence of a lone pair on the C atom substantially diminishes the polarity relative to free CCS, with our calculations suggesting at the highest levels of theory that μ_a is vanishingly small, comparable to that of CO.

With respect to the rotational constants, larger basis sets tend to lead to bond length contraction, which in turn decreases the three moments of inertia, and increases the magnitude of these constants, as Table 1 illustrates. The fractional increase in the rotational constants with respect to the size of the basis set is similar for all three constants (of the order of 2.5 % change between cc-pCVDZ and cc-pCVTZ and 0.5 % between cc-pCVTZ and cc-pCVQZ). However, owing to the much larger value of the A constant, even small fractional differences still correspond to large changes in its magnitude. For example, A_e changes by ∼600 MHz between cc-pCVTZ and cc-pCVQZ, while B_e and C_e only differ about 30 MHz with respect to the same two basis sets. Not withstanding the small μ_a for HCCSH, quite reliable estimates of its low-frequency a-type lines (which scale as integer multiples of

$B + C$) can be made, but much larger and therefore time-consuming searches are required to detect its high-frequency b-type lines (which are roughly $A + C$). Despite the small μ_a, a key advantage of FT microwave spectroscopy is that line intensities scale as μ as opposed to μ^2 in conventional absorption or emission spectroscopy, allowing weak polar species to be routinely detected by this technique.

Table 1: Equilibrium rotational constants (in MHz) of HCCSH following optimization at the ae-CCSD(T)/cc-pCVXZ (X = D, T, Q) level. Dipole moments are evaluated using the CCSD(T)/cc-pCVQZ equilibrium geometry, and their absolute magnitudes are given in Debye. The last two columns indicate the fractional changes of the rotational constants as the size of the basis set increases.

	cc-pCVDZ	cc-pCVTZ	cc-pCVQZ	D → T	T → Q
A_e	285850	292903	293556	2.4%	0.2%
B_e	5372	5513	5545	2.6%	0.6%
C_e	5273	5411	5443	2.6%	0.6%
μ_a	0.03	0.09	0.13		
μ_b	0.90	0.82	0.80		

Laboratory investigation of the HCCSH rotational spectrum

From the *ab initio* structure, the three lowest a-type transitions; $J = 1_{01} - 0_{00}$ ($J = 1 - 0$), $2_{02} - 1_{01}$ ($2 - 1$), and $3_{03} - 2_{02}$ ($3 - 2$), predicted at roughly 11, 22, and 33 GHz, respectively, lie well within the frequency range of our FT microwave spectrometer. A search for the fundamental a-type transition was undertaken first, and soon after yielded an unidentified line within a few MHz of our best estimate (at 10,985 MHz compared to the predicted value of 10,988 MHz from the equilibrium constants, see Table 1). Subsequent screening tests have established that i) this spectral feature requires an electrical discharge; ii) its line intensity is insensitive to the presence of an external magnetic field; and iii) it requires both precursor gases, H_2S and HCCH. Furthermore, the line intensity is maximized at high microwave powers, implying the carrier has a small dipole, which we roughly estimate to be ≤ 0.5 D. Surveys for the next two rotational transitions each resulted in an unidentified

line, systematically offset in frequency from the rigid rotor prediction — i.e. neglecting centrifugal distortion (Figure 3). These two new lines behave in the same manner as the line at 10,985 MHz, and the frequencies of all three are well reproduced (RMS: 0.2 kHz) using a linear molecule Hamiltonian with one free parameter $(B+C)/2$. The best-fit value is within 2% of the *ab initio* prediction for $B+C/2$.

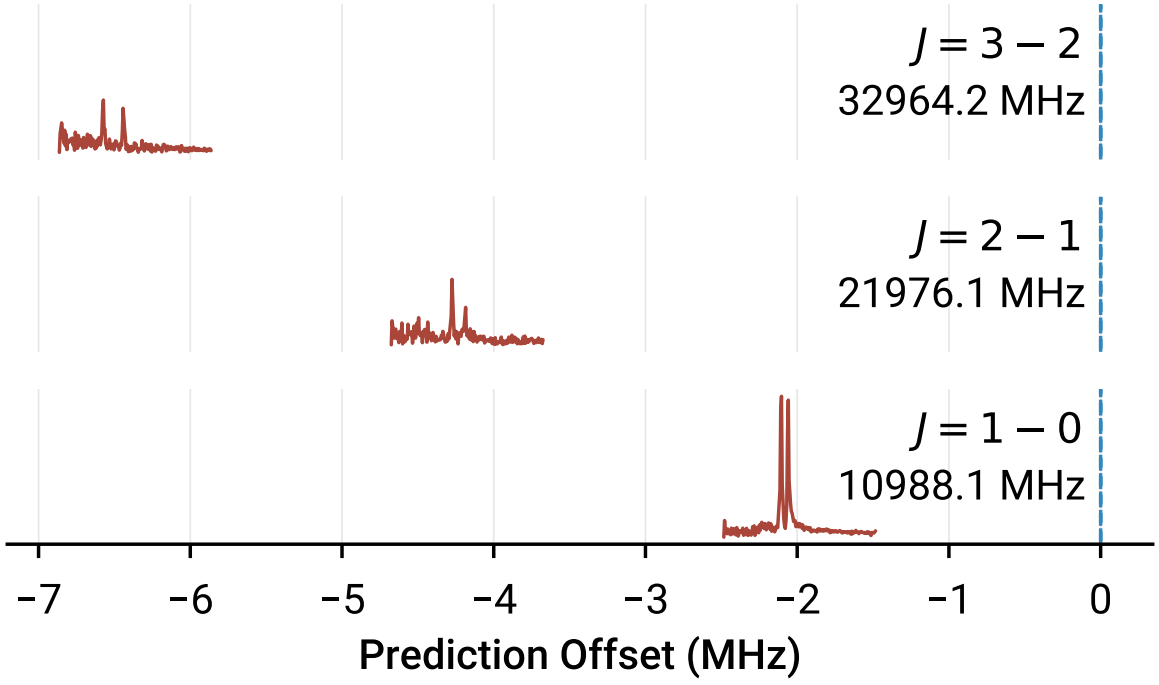

Figure 3: Illustration of the searches conducted for the lowest, *a*-type transitions of HCCSH. The blue lines indicate the *ab initio* predictions based on a harmonic $J'(B_e+C_e)$ approximation, and the red traces show transitions observed consistently offset from the *ab initio* prediction. The doublet structure of the lines is due Doppler splitting, and arises from the co-linear configuration of the cavity axis with respect to that of the supersonic expansion.

To identify the carrier of the new molecule, ostensibly HCCSH, with greater confidence, searches for its isotopologues, the most intense based on natural abundance is ^{34}S (4.21%), were performed. Soon afterwards, a weak line corresponding to the $J = 1-0$ transition of HCC^{34}SH was found within 1 MHz of the frequency predicted by scaling the theoretical rotational constants (see the supplementary material), as were the $J = 2-1$ and $3-2$ lines at higher frequency. In addition, by substituting HCCH with DCCD, and subsequently H_2S

with D_2S, lines of both DCCSH and HCCSD were also observed very close in frequency to the predictions. In the spectra of both, the presence of partially or well-resolved hyperfine-splitting structure arising from the deuteron (Fig. 4) lends further support that the carrier of the new lines is HCCSH or one of its isotopologues, and no other molecule. Finally, by using a statistical mixture of HCCH, $H^{13}CCH$, and $H^{13}C^{13}CH$ as well as pure $H^{13}C^{13}CH$, all possible ^{13}C variants were also detected, namely $H^{13}CCSH$, $HC^{13}CSH$, and $H^{13}C^{13}CSH$. The transition frequencies for all the HCCSH isotopologues measured in the course of the present work are summarized in the supplementary material.

Although we can be confident from the centimeter-wave measurements that HCCSH has been identified, this data alone provides only fragmentary information on the underlying rotational constants, and provides little predictive power of the higher-frequency spectrum, particularly its intense b-type transitions. For these reasons, a search for low-J, b-type lines was initiated using double resonance. Although the predicted transition frequency ($\sim 298\,\mathrm{GHz}$) of the fundamental b-type line ($1_{1,1} - 0_{0,0}$) lies far above the operating range in the FT microwave spectrometer, the lower level in this transition ($0_{0,0}$) is also the lower level of the fundamental a-type transition. Hence, by monitoring the a-type line as the frequency of the millimeter-wave radiation is varied, it should be possible to detect a depletion of its intensity, provided enough millimeter-wave power is available to saturate the high-frequency transition. Although initial surveys close to the predicted frequency of 298 GHz, were unsuccessful, eventually a clear depletion was detected nearly 2 GHz lower in frequency, as depicted in Figure 5, a difference which reflects the large relative uncertainty inherent in the prediction of the A constant. Ultimately, two other b-type transitions were measured in the same fashion, as were an analogous set of lines for HCCSD. By combining the millimeter-wave and centimeter-wave measurements, it was possible to determine preliminary values for all three rotational constants.

From frequency predictions derived from these best-fit constants, the spectroscopy of HCCSH has been extended into the millimeter and submillimeter regime using a frequency

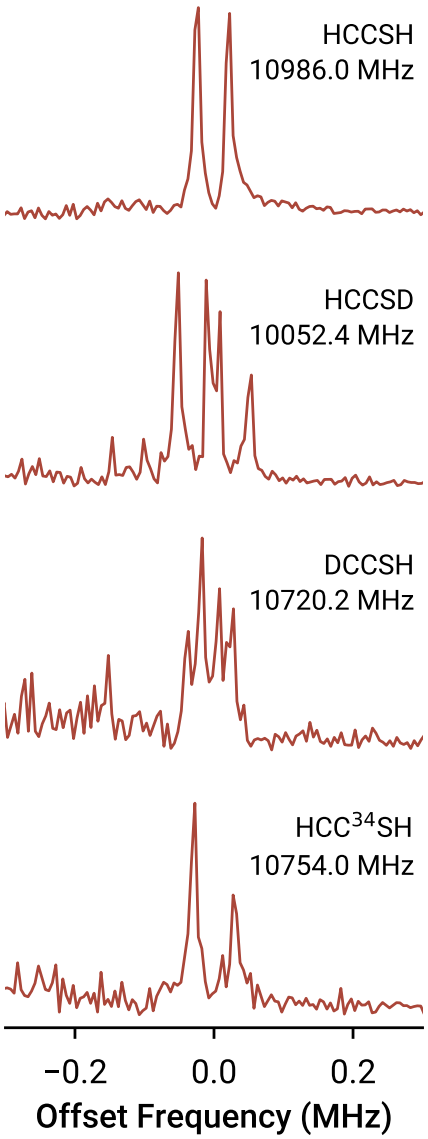

Figure 4: Representative spectra of the fundamental $J = 1 - 0$ transition for HCCSH, HCCSD, DCCSH, and HCC^{34}SH. The rest frequency (used to calculate the offset frequency in the abscissa) of each transition is indicated. In addition to Doppler splitting, partially- or well-resolved hyperfine splitting is apparent in the spectra of the two deuterated species.

multiplication absorption spectrometer. Because many levels are thermally populated in the room temperature radio-frequency discharge source, it was straightforward to measure many b-type lines in this spectral region. In total, an additional 93 lines up to the $^{r}R_0(36)$ and $^{r}Q_0(67)$ were assigned.

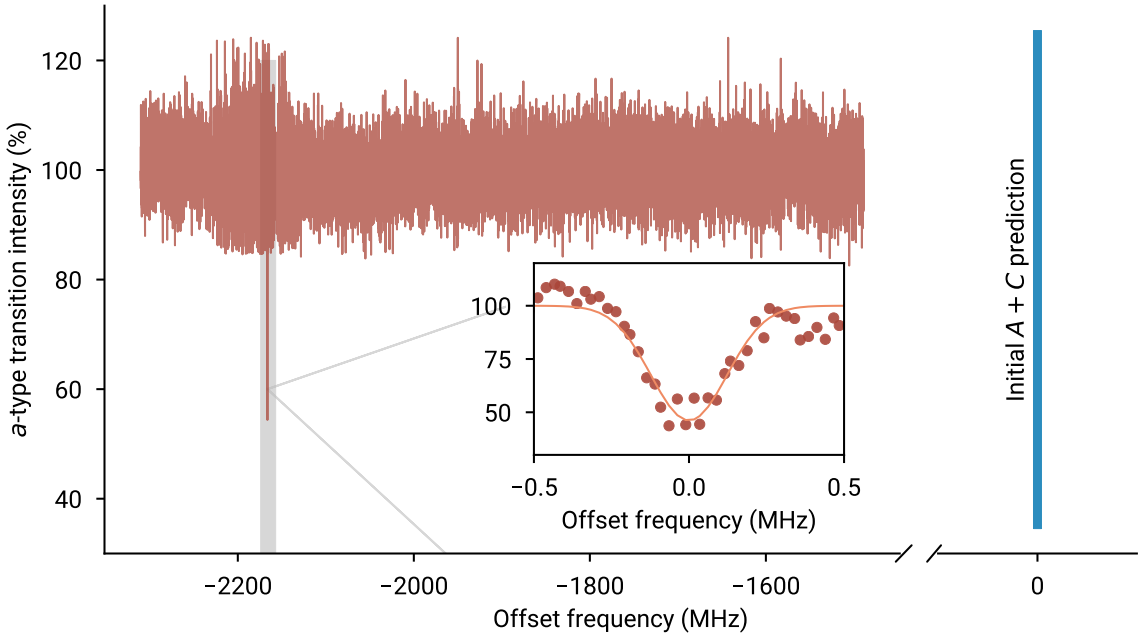

Figure 5: A portion of the double resonance survey for the fundamental b-type transition ($J = 1_{11} - 0_{00}$) of HCCSH, performed by monitoring the intensity of its a-type line at 10,985 MHz ($J = 1_{01} - 0_{00}$). The full survey (2.5 GHz) required more than 72 hours to complete, over which the signal intensity shows fluctuations with time. The initial prediction (indicated by the blue line) was derived from the *ab initio* A and C constants, and the survey was acquired by scanning to lower frequency. The inset shows a higher resolution (50 kHz step size) scan over the transition, showing a clear ($\sim$50%) depletion. The Gaussian fit yields a full-width half-maximum linewidth of 225 kHz, evidence that the depletion is a true molecular resonance and not an instrumental artifact.

Determination of the spectroscopic parameters

Spectroscopic parameters were determined using the SPFIT/SPCAT suite of programs.[40] Owing to the highly prolate character of HCCSH ($\kappa = -0.999$) and the similar magnitudes of B and C, a Watson-S Hamiltonian in the I^r representation was employed. For the main isotopic species, a total of 9 free parameters were required to reproduce the available data to an RMS of 46 kHz (Table 2). In addition to the three rotational constants, three of the five quartic centrifugal distortion terms were varied, as was one sextic (h_1) off-diagonal term, while D_K and d_2 were constrained to their *ab initio* values. As indicated in Table 2, the *ab initio* equilibrium constants are in extremely good agreement with the experimentally-derived ground state constants, within 1% or less. When comparison is possible, the experimental centrifugal distortion constants are also in good agreement with the *ab initio* values. The experimentally-derived inertial defect (0.093 amu Å^2 for HCCSH and 0.0129 amu Å^2 for HCCSD) is consistent with a planar geometry, as expected from the *ab initio* calculations.

Table 2: Spectroscopic parameters for HCCSH obtained by fitting the rotational transition frequencies to a S-reduced Hamiltonian. For comparison, the ae-CCSD(T)/cc-pCVQZ equilibrium rotational constants and quartic centrifugal distortion constants are provided together with the error on these predictions expressed in percentage of the experimental value [$\delta = (exp. - calc.)/calc * 100$]. Parameters are given in units of MHz; values in parentheses correspond to 1σ uncertainty.

Parameter	Experimental fit	*Ab initio*	δ /%
A	291414.3456 (227)	293555.696	−0.73
B	5547.54114 (37)	5545.43900	0.04
C	5438.44470 (34)	5442.62463	−0.08
$D_J \times 10^3$	1.38140 (188)	1.3290	4.99
D_{JK}	0.136695 (139)	0.13925	−0.01
D_K	19.8358[a]	19.8358	
$d_1 \times 10^6$	−0.029306 (45)	−0.24834	15.11
$d_2 \times 10^6$	−3.20926[a]	−3.20926	
$h_1 \times 10^9$	0.1249 (77)		

[a] Value fixed to the CCSD(T)/cc-pCVQZ value

The best-fit spectroscopic constants for all six rare isotopic species are reported in the

supplementary material. Owing to the small number of measured rotational transitions for most of these species, a complete spectroscopic analysis was not feasible. In these cases, some rotational constants were fixed to the corresponding *ab initio* value scaled by the ratio between the experimental and *ab initio* values for the same constant of the main isotopic species, while the centrifugal distortion parameters were fixed to the purely *ab initio* values.

Formation Chemistry

To establish if there is a clear and dominant mechanism responsible for HCCSH in our discharge nozzle, a systematic series of isotopic labelling studies were performed using our FT microwave spectrometer. The strong preferential production of HCCSD when D_2S was used in place of H_2S as a precursor gas, and the absence of detectable quantities of HCCSH when CS_2 is used as an alternative source of sulfur, provide very strong evidence that the SH radical plays a central role in molecule formation.

To explore the formation mechanism in greater detail, two different sources of ^{13}C were also tested: a statistical mixture of $^{12}C/^{13}C$ acetylene (i.e. roughly 25% HCCH, 50% $H^{13}CCH$, and 25% $H^{13}C^{13}CH$), and roughly equal mixtures of normal acetylene (HCCH) and ^{13}C-acetylene ($H^{13}C^{13}CH$). Figure 6 shows the assay matrix, in which the fundamental rotational transition of each $^{12}C/^{13}C$ species was sequentially measured using the two hydrocarbon mixtures. As illustrated in this Figure, lines of all four ^{13}C species were readily detected with the statistical sample. With equal mixtures of HCCH and $H^{13}C^{13}CH$, however, only HCCSH and $H^{13}C^{13}CSH$ were readily observed as discharge products, implying that there is little or no scrambling of the carbon atoms and that the C_2 unit remains intact during molecule formation. In combination with the preferential formation of DCCSH using DCCD as a precursor, we conclude with a high degree of confidence that the reaction most likely involves the C_2H radical. Taken together, all of the available isotopic data is consistent with a simple and direct pathway to form HCCSH in our discharge: homolytic cleavage of the H–S bond of H_2S and the H–C bond in acetylene, followed by radical-radical recombination.

This conclusion is supported by HEAT345(Q) calculations, with the individual contributions organized in Table 3. The total HEAT energies are used to calculate the standard 0 K reaction enthalpy for SH + CCH $\longrightarrow$ HCCSH, which is determined to be -477.2 kJ/mol with a nominal statistical uncertainty of ± 1 kJ/mol.[41] This value is in qualitative agreement with the lower level estimations by Yamada et al.[7], who used B3LYP geometries and zero-point energies combined with CCSD(T)/aug-cc-pVTZ energies to obtain a value of -436 kJ/mol.

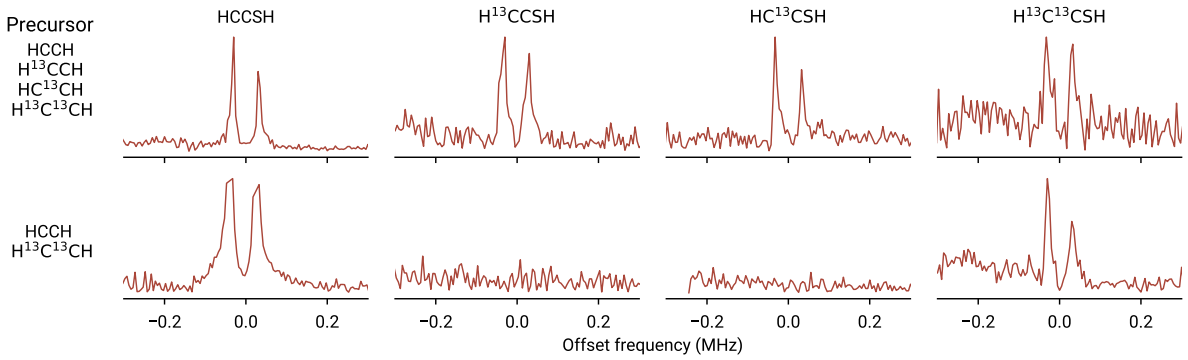

Figure 6: Carbon-13 enriched assays of HCCSH and its isotopologues using two hydrocarbon samples. Each spectrum displays the $J = 1 - 0$ transition of the four ^{13}C species of HCCSH, displayed as an offset with respect to its rest frequency as listed in the SI. The top row indicates the results obtained with a statistical mixture of carbon-13 enriched HCCH, while the bottom row is the same set of measurements, but with a mixture of pure HCCH and H^{13}C^{13}CH. Each scan was accumulated for one minute at a collection rate of 5 Hz.

The molecular structure of HCCSH

Because a large number of isotopic species have been observed in the present work, it is possible to derive both experimental (r_0) and semi-experimental (r_e^{se}) structures for HCCSH. In either structural determination, the six unique structural parameters, the four bond lengths, and the two bond angles (CCS and CSH) as depicted in Fig. 2, were optimized using a standard non-linear least-squares minimization procedure[42] to reproduce to the nine moments of inertia of all seven isotopic species. A planar structure was assumed. For the r_0 structure, B and C for both HCCSH and HCCSD (Table 2) along with $B+C$ for the remain-

Table 3: Breakdown of the contributions to the HEAT345(Q) energy for C_2H, SH, and HCCSH. Energies are given in Hartrees. [MAM: OK for me, but I think in the text you should first report the value in hartree, and refer to the Table, and then it's conversion to kJ/mol]

Contribution	HCCSH	SH	C_2H
SCF/CBS	-474.410257	-398.110854	-76.183645
CCSD(T)/CBS	-1.132275	-0.639181	-0.430304
ZPE	0.027522	0.006224	0.014876
MVD	-1.143031	-1.111314	-0.032137
HLC-(T)	-0.582541	-0.204518	-0.315919
HLC-T	-0.582475	-0.205373	-0.317067
CCSDT(Q)[a]	-0.000929	-0.000120	-0.000611
DBOC	0.009462	0.005953	0.004008
T - (T)[b]	0.000066	-0.000855	-0.001148
HEAT345(Q)	-476.649442	-399.850147	-76.628962

[a] Correlation contribution from fc-CCSDT(Q)/cc-pVDZ
[b] Difference in the extrapolated fc-CCSD(T) and fc-CCSDT energy

ing isotopic species are used, while for the r_e^{se} structure, these constants are first corrected for zero-point vibrational motion, as calculated theoretically using second-order vibrational perturbation theory (VPT2).[43,44] The corrected rotational constants are derived using the equation: $B_e \approx B_0 + \alpha_0$, where α_0 are vibration-rotation interaction constants to first order, which are calculated at the fc-CCSD(T)/ANO0 level of theory (See supplementary material). For normal HCCSH, correction of the three rotational constants reduces the inertial defect from 0.093 to 0.011 amu Å^2, suggesting both the electronic structure method and second-order vibrational perturbation theory accurately treat the vibrational structure.

Table 4 summarizes the best-fit structural parameters in comparison the purely *ab initio* geometry (r_e^{theo}). Although all seven parameters were determined in the r_e^{se} structure, it is not possible to determine the small predicted departure of the CCS angle from linearity in the r_0 structure, so this angle was simply fixed at the theoretical value. This difference aside, the two experimental structures are very similar: the heavy atom bond lengths are not statistically different, but as might be expected when vibrational corrections are included,

both the S–H and C–H bonds contract slightly from the r_0 to the r_e^{se} structure.

The r_e^{se} remarkably well reproduces the available isotopic data: all nine constants are reproduced to better than 0.06 MHz, resulting in statistical uncertainties in the sub-mÅ range for the bond lengths. Furthermore, this structure and the equilibrium structure calculated with theory are in near perfect agreement: differences among the four bond lengths amount to no more than 2 mÅ, while the differences between the two angles are at most 0.6°.

Table 4: The experimental (r_0) and semi-experimental (r_e^{se}) structures, in comparison to the equilibrium structure obtained at the ae-CCSD(T)/cc-pCVQZ level (r_e^{theo}).

Parameter[a]	r_0	r_e^{se}	r_e^{theo}
r_{HC}	1.056(1)	1.0627(1)	1.062
r_{CC}	1.209(3)	1.2082(3)	1.208
r_{CS}	1.691(2)	1.6892(2)	1.691
r_{SH}	1.366(2)	1.3403(4)	1.338
θ_{CCS}	175.5[b]	174.93(18)	175.5
θ_{CSH}	95.33(15)	96.04(5)	96.2

[a] Bond lengths in Angstroms, bond angles in degrees. Values in parentheses are formal 1σ statistical uncertainties.

[b] Fixed to the *ab initio* equilibrium value.

Stability and relative abundances of the [H_2,C_2,S] isomers

The re-computed relative energies of the three lowest energy [H_2,C_2,S] isomers are shown in Figure 1. The values derived here are in qualitative agreement with those obtained with the latest MP2/6-311G(2d,p) and B3LYP/6-311G(2d,p) calculations by Frolov et al. [4], and other calculations. [7] In all cases, the energy ordering of the three isomers is identical, however, there are quantitative differences in the relative energetics. For HCCSH, the B3LYP determination (76.2 kJ/mol) is much larger than that derived from the MP2 calculations (56.6 kJ/mol) by Frolov et al. [4], while the MP2 prediction is very close to the HEAT345(Q) value (56.3 kJ/mol). This small difference is likely fortuitous, owing to a cancellation of errors, as the same agreement is not observed for *c*-H_2C_2S. The HEAT345(Q) calculations predict that *c*-H_2C_2S

is much more stable (132.1 kJ/mol) either compared to the MP2 (145.3 kJ/mol) or B3LYP (155.2 kJ/mol) predictions.[4] We attribute this stability to the improved treatment of dynamic correlation by coupled-cluster methods, combined with much larger basis sets used in the present calculation.

H_2CCS and HCCSH are observed with comparable intensity in our electrical discharge when H_2S is used as the source of sulfur. Because H_2CCS is much more polar than HCCSH (μ_a= 1.02 vs. 0.13 D),[45] however, this implies that HCCSH was roughly four times more abundant under these conditions, taking into account nuclear spin statistics and differences in the rotational partition function. When CS_2 is used instead of H_2S, lines of H_2CCS are observed with similar intensity, while those of HCCSH are no longer detectable. With respect to H_2CCS formation, these results suggest the importance of atomic sulfur. Although speculative, this finding is consistent with two pathways suggested by Yamada et al.:[7] the reaction H + HCCS, where HCCS is presumably formed by the reaction HCC + S; or CH + HCS. Because one pathway conserves the C_2 unit in molecule formation, while the other does not, analogous ^{13}C isotopic studies to those performed here should prove highly informative in clarify the pathways that yield thioketene from either H_2S and CS_2.

Prospects for detection of higher-energy isomers

A combination of discharge sources and supersonic jets has been used extensively to study higher-energy isomers,[46–49] and HCCSH is no exception. Under some experimental conditions, HCCSH is produced much more efficiently than the ground state isomer H_2CCS, despite the much lower stability of the former (56 kJ/mol). The implication of this and previous studies is that collisional cooling near the throat of the expansion is fast relative to the timescale for unimolecular isomerization. The efficiency of "trapping" energetic isomers appears particularly high when isomerization barriers are substantial, as has previously been calculated for HCCSH $\leftrightarrow$ H_2CCS interconversion ($\sim$80 kJ/mol; Ref. 50). These results are in sharp contrast to the mechanisms at play in cryogenic matrices.[5,6] In previous studies

in argon matrices following UV irradiation of thiadazoles, it was found that H_2CCS formed first, and subsequent isomerization produced higher-energy species such as HCCSH and c-H_2C_2S. At sufficiently long time scales however, HCCSH is thought to rapidly tautomerize to H_2CCS.[8]

The present work suggests gas-phase detection of thiirene *c*-H_2C_2S should be feasible with our FT microwave spectrometer. Theoretical calculations[7] also conclude that once formed, there are sizable isomerization barriers (of order 100 kJ/mol) to either H_2CCS or *c*-H_2CCS. Given i) the high abundance of HSCCH that can be achieved; ii) the high accuracy with which the rotational spectrum of *c*-H_2C_2S can likely be predicted; and iii) its high polarity, it would be surprising —perhaps even disappointing— if the rotational spectrum of this small, elusive antiaromatic heterocycle is not eventually be found.

Astronomical implications

Because there is very strong evidence the SH + CCH reaction is responsible for HCCSH in our discharge nozzle, and because the HEAT345(Q) energetics confirm this reaction is highly exothermic (-477 kJ/mol), it is conceivable this metastable isomer might form preferentially in the interstellar medium, especially so since both the SH and CCH radicals are widely abundant and widely distributed there. If relevant, this mechanism should be efficient even in low temperature environments such as dark molecular clouds ($\sim$20 K) which may make HCCSH a viable sink of sulfur content there, a particularly intriguing possibility since this element is known to heavily depleted in these regions.[51–53]

With the spectroscopic constants listed in Table 2, it is possible to predict the astronomically most interesting lines over the entire range of interest to radio astronomers. Of particular importance is the strong *b*-type lines, which can now be predicted to better than 0.1 km sec^{-1} in terms of equivalent radio velocity up to 800 GHz. With this data, evidence for HCCSH can be sought in published line surveys of rich molecular sources, and dedicated searches can now be undertaken with confidence as well using powerful, high-altitude

interferometers such as the Atacama Large Millimeter Array.

Conclusions

A high-resolution study on the gas-phase rotational spectrum of HCCSH, the second most stable isomer with the elemental formula [H_2,C_2,S] was carried out. By measuring a total of 100 pure rotational transitions using on a combination of Fourier-transform microwave and submillimeter-wave spectroscopies guided by high level *ab initio* predictions, its rotational spectrum has been characterized from 10 to 660 GHz. Accurate spectroscopic parameters have been determined from a fit of the experimental frequencies to a standard asymmetric top Hamiltonian with up to sextic centrifugal distortion constants. The identity of HCCSH was confirmed by detecting several microwave rotational transitions of six rare isotopic species: DCCSH, HCCSD, HCC^{34}SH, H^{13}CCSH, HC^{13}CSH, and H^{13}C^{13}CSH. The isotopic measurements were beneficial in two other ways: to determine the molecular structure of HCCSH, and to infer its formation pathway in the electrical discharge, which we deduce to be radical recombination of SH + C_2H $\rightarrow$ HCCSH. This reaction is highly exothermic (-477 kJ/mol), as determined with the HEAT345(Q) method. The relative energetics of the [H_2,C_2,S] isomers have also been determined to higher accuracy compared to previously published methods.

With accurate predictions for transition frequencies of HCCSH up to about 1 THz, astronomical searches for this molecule can now be undertaken with confidence. While HCCSH is not the ground state isomer, considering it is preferentially formed via radical-radical recombination of two abundant interstellar species — namely SH and C_2H — and that kinetics rather than thermodynamic considerations often prevail in interstellar chemistry, this isomer appears to be a good candidate for astronomical detection. Using the same laboratory techniques, detection of *c*-H_2C_2S would appear promising.

Acknowledgements

We thank Edward Tong of the Submillimeter Array Receiver laboratory at the Smithsonian Astrophysical Observatory for the loan of a high-power, high-frequency VDI AMC that was used for the 300 GHz DR measurements. Support for B.A.M. was provided by NASA through Hubble Fellowship grant #HST-HF2-51396 awarded by the Space Telescope Science Institute, which is operated by the Association of Universities for Research in Astronomy, Inc., for NASA, under contract NAS5-6555. The National Radio Astronomy Observatory is a facility of the National Science Foundation operated under cooperative agreement by Associated Universities, Inc. The work in Cambridge is supported by NSF AST-1615847.

Supplemntary material

Tables of frequencies for observed transitions, spectroscopic parameters used in the structure determination, and additional theoretical data can be found in supplementary material.

References

(1) Siegbahn, P. E. M.; Yoshimine, M.; Pacansky, J. A theoretical study of the lowest singlet and triplet surfaces of C_2H_2S. *The Journal of Chemical Physics* **1983**, *78*, 1384–1389.

(2) Carsky, P.; Andes Hess, B.; Schaad, L. J. Ab initio study of the structures and vibrational spectra of the Hueckel 4n heterocycles azirine, oxirene and thiirene. *Journal of the American Chemical Society* **1983**, *105*, 396–402.

(3) Bouma, W. J.; Nobes, R. H.; Radom, L.; Woodward, C. E. Existence of stable structural isomers of ketene. A theoretical study of the C_2H_2O potential energy surface. *The Journal of Organic Chemistry* **1982**, *47*, 1869.

(4) Frolov, Y. L.; Malkina, A. G.; Trofimov, B. A. Isomer structures of thioketene and

its cyclic oligomers. Ab initio calculations. *Journal of Structural Chemistry* **2005**, *46*, 28–33.

(5) Krantz, A.; Laureni, J. Characterization of matrix-isolated antiaromatic three-membered heterocycles. Preparation of the elusive thiirene molecule. *Journal of the American Chemical Society* **1981**, *103*, 486–496.

(6) Krantz, A.; Laureni, J. Matrix photolysis of 1,2,3-thiadiazole. Possible involvement of thiirene. *Journal of the American Chemical Society* **1974**, *96*, 6768–6770.

(7) Yamada, M.; Osamura, Y.; Kaiser, R. I. A comprehensive investigation on the formation of organo-sulfur molecules in dark clouds via neutral-neutral reactions. *Astronomy & Astrophysics* **2002**, *395*, 1031–1044.

(8) Schaumann, E. The chemistry of thioketens. *Tetrahedron* **1988**, *44*, 1827–1871.

(9) Kroto, H. W.; McNaughton, D. Fourier transform infrared spectrum of thioketen, CH_2=C=S. *Journal of Molecular Spectroscopy* **1985**, *114*, 473–482.

(10) Jarman, C. N.; Kroto, H. W. High-resolution Fourier-transform Infrared Spectroscopy of $v_3 + v_8$ H_2CCS, v_1 HDCCS and v_1 D_2CCS in the Gas Phase: an Improved r_s Structure for Thioketene. *Journal of the Chemical Society, Faraday Transactions* **1991**, *87*, 12.

(11) Torres, M.; Lown, E. M.; Gunning, H. E.; Strausz, O. P. 4n-π electron antiaromatic heterocycles. *Pure & Applied Chemistry* **1980**, *52*, 1623–1643.

(12) Braslavsky, S.; Heicklen, J. The gas-phase thermal and photochemical decomposition of heterocyclic compounds containing nitrogen, oxygen, or sulfur. *Chemical Reviews* **1977**, *77*, 473.

(13) Burdzinski, G.; Luk, H. L.; Reid, C. S.; Zhang, Y.; Hadad, C. M.; Platz, M. S. The Photochemistry of 4,5-Carbomethoxy-1,2,3-thiadiazole: Direct Observation of Thiirene

Formation and Its Decay in Solution. *The Journal of Physical Chemistry A* **2013**, *117*, 4551–4555.

(14) Burdzinski, G.; Sliwa, M.; Zhang, Y.; Delbaere, S.; Pedzinski, T.; Rhault, J. Photochemical formation of thiirene and thioketene in 1,2,3-thiadiazoles with phenyl substituents studied by time-resolved spectroscopy. *Photochemical & Photobiological Sciences* **2013**, *12*, 895.

(15) Loomis, R. A.; McGuire, B. A.; Shingledecker, C.; Johnson, C. H.; Blair, S.; Robertson, A.; Remijan, A. J. Investigating the minimum energy principle in searches for new molecular species—the case of H_2C_3O isomers. *The Astrophysical Journal* **2015**, *799*, 34–8.

(16) Yamamoto, S.; Saito, S.; Kawaguchi, K. Laboratory detection of a new carbon-chain molecule C_3S and its astronomical identification. *The Astrophysical Journal* **1987**, *317*, L119.

(17) Gordon, V. D.; McCarthy, M. C.; Apponi, A. J.; Thaddeus, P. Rotational Spectra of Sulfur-Carbon Chains. I. The Radicals C_4S, C_5S, C_6S, C_7S, C_8S, and C_9S. *The Astrophysical Journal Supplement Series* **2001**, *134*, 311.

(18) McGuire, B. A.; Martin-Drumel, M. A.; Lee, K. L. K.; Stanton, J. F.; Gottlieb, C. A.; McCarthy, M. C. Vibrational satellites of C_2S, C_3S, and C_4S: microwave spectral taxonomy as a stepping stone to the millimeter-wave band. *Physical Chemistry Chemical Physics* **2018**, *20*, 13870–13889.

(19) Gordon, V. D.; McCarthy, M. C.; Apponi, A. J.; Thaddeus, P. Rotational Spectra of SulfurCarbon Chains. II. HC_5S, HC_6S, HC_7S, and HC_8S, and H_2C_4S, H_2C_5S, H_2C_6S, and H_2C_7S. *The Astrophysical Journal Supplement Series* **2002**, *138*, 297–303.

(20) Hirahara, Y. Pulsed-discharge-nozzle Fourier-transform microwave spectroscopy of HC_3S ($^2\Pi_r$) and HC_4S ($^2\Pi_i$). **1994**, *101*, 9.

(21) Stanton, J. F.; Gauss, J.; Cheng, L.; Harding, M. E.; Matthews, D. A.; Szalay, P. G. CFOUR, Coupled-Cluster techniques for Computational Chemistry, a quantum-chemical program package. 2017.

(22) Stanton, J. F. Why CCSD(T) works: a different perspective. *Chemical Physics Letters* **1997**, *281*, 130–134.

(23) Bartlett, R. J.; Watts, J. D.; Kucharski, S. A.; Noga, J. Non-iterative fifth-order triple and quadruple excitation energy corrections in correlated methods. *Chemical Physics Letters* **1990**, *165*, 513–522.

(24) Raghavachari, K.; Trucks, G. W.; Pople, J. A.; Head-Gordon, M. A fifth-order perturbation comparison of electron correlation theories. *Chemical Physics Letters* **1989**, *157*, 479–483.

(25) Woon, D. E.; Dunning, T. H. Gaussian basis sets for use in correlated molecular calculations. III. The atoms aluminum through argon. *The Journal of Chemical Physics* **1993**, *98*, 1358–1371.

(26) Woon, D. E.; Dunning, T. H. Gaussian basis sets for use in correlated molecular calculations. V. Corevalence basis sets for boron through neon. *The Journal of Chemical Physics* **1995**, *103*, 4572–4585.

(27) Dunning, T. H. Gaussian basis sets for use in correlated molecular calculations. I. The atoms boron through neon and hydrogen. *The Journal of Chemical Physics* **1989**, *90*, 1007–1023.

(28) Bomble, Y. J.; Vazquez, J.; Kallay, M.; Michauk, C.; Szalay, P. G.; Csaszar, A. G.; Gauss, J.; Stanton, J. F. High-accuracy extrapolated ab initio thermochemistry. II. Minor improvements to the protocol and a vital simplification. *Journal of Chemical Physics* **2006**, *125*, 064108.

(29) Harding, M. E.; Vazquez, J.; Ruscic, B.; Wilson, A. K.; Gauss, J.; Stanton, J. F. High-accuracy extrapolated ab initio thermochemistry. III. Additional improvements and overview. *Journal of Chemical Physics* **2008**, *128*, 114111.

(30) Scuseria, G. E.; Schaefer, H. F. A new implementation of the full CCSDT model for molecular electronic structure. *Chemical Physics Letters* **1988**, *152*, 382–386.

(31) Handy, N. C.; Yamaguchi, Y.; Schaefer, H. F. The diagonal correction to the Born-Oppenheimer approximation: Its effect on the singlet-triplet splitting of CH_2 and other molecular effects. *The Journal of Chemical Physics* **1986**, *84*, 4481–4484.

(32) Cowan, R. D.; Griffin, D. C. Approximate relativistic corrections to atomic radial wave functions. *JOSA* **1976**, *66*, 1010–1014.

(33) Klopper, W. Simple recipe for implementing computation of first-order relativistic corrections to electron correlation energies in framework of direct perturbation theory. *Journal of Computational Chemistry* **1997**, *18*, 20–27.

(34) Kállay, M.; Gauss, J. Approximate treatment of higher excitations in coupled-cluster theory. II. Extension to general single-determinant reference functions and improved approaches for the canonical Hartree-Fock case. *The Journal of Chemical Physics* **2008**, *129*, 144101.

(35) McCarthy, M. C.; Chen, W.; Travers, M. J.; Thaddeus, P. Microwave Spectra of 11 Polyyne Carbon Chains. *The Astrophysical Journal Supplement Series* **2000**, *129*, 611.

(36) Pirali, O.; Goubet, M.; Boudon, V.; D'Accolti, L.; Fusco, C.; Annese, C. Characterization of isolated 1-aza-adamantan-4-one ($C_9H_{13}NO$) from microwave, millimeter-wave and infrared spectroscopy supported by electronic structure calculations. *J. Mol. Spectrosc.* **2017**, *338*, 6 – 14.

(37) Martin-Drumel, M. A.; Pirali, O.; Balcon, D.; Brechignac, P.; Roy, P.; Vervloet, M. High resolution far-infrared Fourier transform spectroscopy of radicals at the AILES beamline of SOLEIL synchrotron facility. *Rev. Sci. Instrum.* **2011**, *82*, 113106.

(38) Meerts, W. L.; Dymanus, A. The Hyperfine Λ-Doubling Spectrum of Sulfur Hydride in the $^2\Pi_{3/2}$ State. *Astrophys. J. Lett.* **1974**, *187*, L45.

(39) Murakami, A. A quantum chemical study on the linear C_2S and C_3S molecules. *Astrophys. J.* **1990**, *357*, 288–290.

(40) Pickett, H. M. The fitting and prediction of vibration-rotation spectra with spin interactions. *Journal of Molecular Spectroscopy* **1991**, *148*, 371–377.

(41) Karton, A. A computational chemist's guide to accurate thermochemistry for organic molecules. *Wiley Interdisciplinary Reviews: Computational Molecular Science* **2016**, *6*, 292–310.

(42) Kisiel, Z. Least-Squares Mass-Dependence Molecular Structures for Selected Weakly Bound Intermolecular Clusters. *J. Mol. Spectrosc.* **2003**, *218*.

(43) Stanton, J. F.; Gauss, J. Analytic second derivatives in high-order many-body perturbation and coupled-cluster theories: Computational considerations and applications. *International Reviews in Physical Chemistry* **2000**, *19*, 61–95.

(44) Schneider, W.; Thiel, W. Anharmonic force fields from analytic second derivatives: Method and application to methyl bromide. *Chemical Physics Letters* **1989**, *157*, 367–373.

(45) Georgiou, K.; Kroto, H.; M. Landsberg, B. The microwave spectrum, substitution structure, and dipole moment of thioketene, H_2CCS. **1979**, *77*, 365–373.

(46) Brnken, S.; Yu, Z.; Gottlieb, C. A.; McCarthy, M. C.; Thaddeus, P. Laboratory Detection of Thiocyanic Acid HSCN. *The Astrophysical Journal* **2009**, *706*, 1588.

(47) McCarthy, M. C.; Thaddeus, P. Laboratory detection of the elusive $HSCO^+$ isomer. *The Journal of Chemical Physics* **2007**, *127*, 221104.

(48) McCarthy, M.; Tamassia, F.; Thorwirth, S. High-resolution rotational spectroscopy of iminosilylene, HNSi. *Molecular Physics* **2015**, *113*, 2204–2216.

(49) Lattanzi, V.; Thorwirth, S.; Gottlieb, C. A.; McCarthy, M. C. Two Isomers of Protonated Isocyanic Acid: Evidence for an Ion-Molecule Pathway for HNCO $\leftrightarrow$ HOCN Isomerization. *The Journal of Physical Chemistry Letters* **2012**, *3*, 3420–3424.

(50) Gosavi, R. K.; Strausz, O. P. Ab initio molecular orbital studies on thiirene and its isomeric structures. *Canadian Journal of Chemistry* **1983**, *61*, 2596–2610.

(51) Boogert, A. C. A.; Schutte, W. A.; Helmich, F. P.; Tielens, A. G. G. M.; Wooden, D. H. Infrared observations and laboratory simulations of interstellar CH_4 and SO_2. *Astronomy & Astrophysics* **1997**, *317*, 929–941.

(52) Bilalbegović, G.; Baranović, G. Sulphur-bearing species in molecular clouds. *Monthly Notices of the Royal Astronomical Society* **2015**, *446*, 3118–3129.

(53) Martín-Doménech, R.; Jimenez-Serra, I.; Muñoz Caro, G. M.; Müller, H. S. P.; Occhiogrosso, A.; Testi, L.; Woods, P. M.; Viti, S. The sulfur depletion problem: upper limits on the H_2S_2, HS_2, and S_2 gas-phase abundances toward the low-mass warm core IRAS 16293-2422. *Astronomy & Astrophysics* **2016**, *585*, A112–9.